Pharmacological Reports (2020) 72:1614–1626
https://doi.org/10.1007/s43440-020-00091-5

ARTICLE

Blockade of the colony-stimulating factor-1 receptor reverses bone loss in osteoporosis mouse models

Arisaí Martínez-Martínez[1] · Enriqueta Muñoz-Islas[1] · Martha B. Ramírez-Rosas[1] · Rosa I. Acosta-González[1] · Héctor F. Torres-Rodríguez[1] · Juan M. Jiménez-Andrade[1]

Received: 20 November 2019 / Revised: 27 January 2020 / Accepted: 19 February 2020 / Published online: 28 March 2020

Abstract

Background Mice lacking either colony-stimulating factor-1 (CSF-1) or its receptor, CSF-1R, display osteopetrosis. Accordingly, genetic deletion or pharmacological blockade of CSF-1 prevents the bone loss associated with estrogen deficiency. However, the role of CSF-1R in osteoporosis models of type-1 diabetes (T1D) and ovariectomy (OVX) has not been examined. Thus, we evaluated whether CSF-1R blockade would relieve the bone loss in a model of primary osteoporosis (female mice with OVX) and a model of secondary osteoporosis (female with T1D) using micro-computed tomography.

Methods Female ICR mice at 10 weeks underwent OVX or received five daily administrations of streptozotocin (ip, 50 mg/kg) to induce T1D. Four weeks after OVX and 14 weeks after first injection of streptozotocin, mice received an anti-CSF-1R (2G2) antibody (10 mg/kg, ip; once/week for 6 weeks) or vehicle. At the last day of antibody administration, mice were sacrificed and femur and tibia were harvested for micro-computed tomography analysis.

Results Mice with OVX had a significant loss of trabecular bone at the distal femoral and proximal tibial metaphysis. Chronic treatment with anti-CSF-1R significantly reversed the trabecular bone loss at these anatomical sites. Streptozotocin-induced T1D resulted in significant loss of trabecular bone at the femoral neck and cortical bone at the femoral mid-diaphysis. Chronic treatment with anti-CSF-1R antibody significantly reversed the bone loss observed in mice with T1D.

Conclusion Our results demonstrate that blockade of CSF-1R signaling reverses bone loss in two different mouse models of osteoporosis.

Keywords Osteoporosis · Colony-stimulating factor-1 · Diabetes · Mouse models · Bone loss prevention

Introduction

Osteoporosis is a major public health problem not only in postmenopausal women (type 1-primary osteoporosis) and people over 70 years old (type 2-primary osteoporosis) but also in people under 70 years and premenopausal women (secondary osteoporosis). In these latter cases, osteoporosis is a consequence of treatments and/or diseases such as diabetes mellitus (DM) [1]. Both primary and secondary osteoporosis are a significant contributor to morbidity, mortality, and lost life years globally. In the USA, osteoporosis and low bone mass combined affected approximately 53.6 million (54%) older adults in 2010 [2].

In the last decades, there has been a remarkable progress in our understanding of the mechanisms behind the development of osteoporosis and new drugs have been discovered to treat the disease. However, there is still an increasing treatment gap for patients with osteoporosis and a high risk

✉ Juan M. Jiménez-Andrade
jimenez.andrade1810@gmail.com

Arisaí Martínez-Martínez
mtz.arisai@gmail.com

Enriqueta Muñoz-Islas
e.munoz.islas@gmail.com

Martha B. Ramírez-Rosas
maberaro@outlook.com

Rosa I. Acosta-González
racosta@uat.edu.mx

Héctor F. Torres-Rodríguez
hftorres@uat.edu.mx

[1] Laboratorio de Farmacología, Unidad Académica Multidisciplinaria Reynosa-Aztlán, Universidad Autónoma de Tamaulipas, Calle 16 y Lago de Chapala, Col. Aztlán, 88740 Reynosa, TAMPS, México

of fracture. This is in part due to concerns about rare side effects such as atypical fractures and osteonecrosis of the jaw (e.g. bisphosphonates) and lack of long-term (> 5 year) efficacy (e.g. bisphosphonates and denosumab) [3]. Even the recently discovered osteoporosis drugs such as parathyroid hormone-related peptide analog, sclerostin antibody and cathepsin K inhibitor have been reported to induce serious adverse effects in clinical phase 3 trials (injection-site reaction, arthralgia, osteonecrosis of the jaw, atypical femoral fracture and stroke [3]). As the life expectancy of humans is increasing, the prevalence of osteoporosis itself and diseases leading to osteoporosis (e.g. DM) will continue to rise in the world [1, 4, 5]. Thus, there is a medical need to develop safer and more efficacious anti-osteoporotic therapies.

Bone remodeling is a highly regulated and dynamic process involving the orchestration of osteoclastic bone resorption and osteoblastic bone formation [6, 7]. An alteration between these anabolic and catabolic events can result in a decreased bone quality and an increased fracture risk. For example, the estrogen loss in women after menopause frequently results in excessive osteoclast formation and bone resorption activity leading to osteoporosis. This process is termed postmenopausal osteoporosis and is the most common type of osteoporosis [8–10].

Apart from the known vascular complications, patients with DM have pathological changes in bone remodeling leading to an increased risk of bone fracture [11]. Several studies have demonstrated that in patients with type 1 diabetes (T1D), there is a ~ 6–17 fold increased risk of hip fractures compared to age-matched people without T1D [12, 13]. While the mechanisms underlying bone loss in T1D are not completely understood, some mouse studies have shown that streptozotocin (STZ)-induced hyperglycemia positively regulates osteoclast differentiation and function through suppression of osteoblast maturation and increases in bone adiposity in long bones [14, 15].

Colony-stimulating factor-1 [CSF-1, also known as macrophage colony-stimulating factor (M-CSF)], released by different cell types including fibroblasts, endothelial cells, and osteoblasts, induces homodimerization and subsequent activation of its receptor CSF-1R (also known as c-Fms or CD115) [16, 17]. CSF-1R is expressed predominantly on monocytes, macrophages, myeloid dendritic cells, microglia, and osteoclasts. CSF-1R regulates the survival, proliferation, differentiation, and function of monocyte lineage cells, including macrophages and osteoclasts (bone resorption cells) [18]. Several studies have shown a pivotal role of the CSF-1/CSF-1R pathway in pathological bone resorption [19]. Mice lacking either CSF-1 or CSF-1R display osteopetrosis and reduced osteoclastogenesis [20, 21]. Moreover, genetic deletion or pharmacological blockade of CSF-1 prevents ovariectomy (OVX)-induced bone loss. Additionally, increased levels of CSF-1 protein and mRNA have been reported in bone marrow cells isolated from mice with OVX and levels of CSF-1R mRNA expression are significantly increased in cultured macrophages under hyperglycemia stages [22]. Finally, levels of CSF-1 in bone marrow cells positively correlate with number of osteoclasts [23] and very recently, it has been reported that a CSF-1R inhibitor (PLX3397) significantly abolished the LPS-induced bone microstructure damage [24]. Altogether, these results suggest that CSF-1/CSF-1R axis is involved in the pathogenesis of bone loss associated with OVX and T1D. Therefore, we aimed to determine the effect of a blocking anti-CSF-1R antibody on both cortical and trabecular bone in two accepted murine models of primary (OVX-induced bone loss) and secondary (STZ-induced T1D) osteoporosis using micro-computed tomography analysis.

Materials and methods

Animals

Experiments were performed on a total of 54 female ICR mice obtained from Envigo Laboratories (Mexico City, Mexico) weighing 25–30 g (10 weeks old) at the beginning of the experiments. The sample size was based on previous studies in our laboratory [25, 26]. Animals were randomly selected and divided into two experimental groups (OVX and T1D). OVX group ($n = 24$) was subdivided into four groups, naïve ($n = 6$), sham ($n = 6$), OVX + vehicle (Veh) ($n = 6$), OVX + 2G2 ($n = 6$), while T1D group ($n = 23$) was subdivided into three groups, citrate ($n = 7$), STZ + Veh ($n = 7$), STZ + 2G2 ($n = 9$). Additionally, a group of age-matched naïve mice was treated with 2G2 ($n = 7$). Efforts were made to minimize the number of animals used. Mice were housed in groups of four per cage at a constant temperature of 22 °C ± 2 °C and a 12-h light/dark cycle, with access to food (standard diet, catalog no. 2016S) and water ad libitum. Procedures involving mice and their care were conducted in conformity with the Mexican Official Norm for Animal Care and Handling (NOM-062-ZOO-1999) and the Guide for the Care and Use of Laboratory Animals. All animal procedures were approved by Animal Ethics Committee of the Universidad Autónoma de Tamaulipas (CEI-UAMRA-2016-0015).

Model of primary osteoporosis

Primary osteoporosis was induced in mice by performing a bilateral OVX at 10 weeks of age. Briefly, bilateral OVX or sham surgery (Sham) under ketamine/xylazine anesthesia (50/5 mg/kg, sc) were performed. Mice were placed in prone position and shaved between the last rib and hip. One-centimeter incision was made in the back on each side, then

the ovaries were located and removed together with their capsule and part of the oviduct. The uterine horns were then sutured with absorbable suture, and the skin was closed with nylon 4–0 suture (Atramat, Nylon). At the end of the recovery (2 weeks after OVX), the success of the surgery was confirmed by vaginal cytology [27].

Model of secondary osteoporosis

Type-1 diabetes-induced osteoporosis was induced at 10 weeks of age. Female mice were daily administrated by intraperitoneal injection for 5 consecutive days with STZ (50 mg/kg in 0.1 M citrate buffer pH 4.5) as previously reported [25]. Control group was injected only with citrate buffer. Two weeks post-first injection, mice were fasted for 12 h and glucose levels were measured in a blood drop obtained from a 1 mm cut made in the distal tail tip using a glucometer (Accutrend Plus CTL., Roche Diagnostic). Mice with blood glucose levels higher than 200 mg/dL were considered as diabetic [25].

Micro-computed tomography analysis

Trabecular bone was analyzed at the level of the distal femur, proximal tibia, and femoral neck. Cortical bone was evaluated at the mid-diaphysis level of the femur and tibia, using micro-computed tomography system (Skyscan 1272, Bruker, Belgium). The scanning process was made at a 10 µm voxel size, an X-ray power of 60 kVp and 166 µA with an integration time of 627 ms, according to the guidelines for microCT analysis for rodent bone structure [28]. Obtained images were reconstructed using NRecon software (Bruker, Belgium). The trabecular region of interest (ROI) at distal femur and proximal tibia metaphysis was evaluated by selecting 2 mm in the vertical axis, subsequent to 0.5 mm from the growth plate (reference point). For the cortical ROI analysis, the sample level was selected a band of 1 mm thick at 4 mm distally from the growth plate. For the femoral neck analysis, ROI was selected using a 0.5 mm^2 cylinder that was positioned in the region of the neck in all analyzed samples. The CT analyzer program (Bruker, Belgium) was used to determine trabecular bone parameters; an automatic segmentation algorithm (CT analyzer) was applied to isolate the trabecular bone from the cortical bone. The parameters used for the trabecular bone were trabecular bone volume rate (BV/TV), trabecular separation (Tb.Sp), trabecular number (Tb.N). Cortical bone parameters in 3D were cortical thickness (Ct.Th) and 2D mean cross-sectional bone area (B.Ar), mean cross-sectional tissue area (T.Ar) and mean cortical area fraction (B.Ar/T.Ar). Finally, hydroxyapatite calibration phantoms (250 and 750 mg/cm^3) were used to calibrate trabecular and cortical bone mineral density values (BMD).

Administration of 2G2

The 2G2 is a chimera hamster and mouse IgG1 antagonistic antibody that binds to mouse CSF-1R with high affinity and enables specific and long-term CSF-1R inhibition in immune-competent mice. The dose of anti-CSF-1R antibody administered in this study was based on previous studies and adjusted to non-tumor bearing mice [29]. Four weeks post-surgery, OVX or sham mice, 14 weeks post-first injection of STZ, or age-matched naïve (14 weeks of age at the beginning of treatment) animals were administered 2G2 (anti-CSF-1R) or vehicle (ip) at the dose of 10 mg/kg once weekly for 6 consecutive weeks (Fig. 1). Based on our pilot studies, anti-CSF-1R was initially given when there was significant bone loss in the distal femur (OVX study) and neck of the femur (T1D study). At the end of the administration, mice were sacrificed using a CO_2 chamber and hind limbs were harvested and stored at 4 °C in 0.1 M PBS (pH 7.4) until their analysis.

Reagents

The compounds used in the present study were Streptozotocin (STZ) (Sigma-Aldrich, catalog #S0130), Citric acid monohydrate (J.T. Baker, catalog #0110-01), Sodium citrate dihydrate (J.T. Baker, catalog #3646-01), antibody against CSF-1R (2G2, kindly provided by Roche Diagnostics GmbH, Germany), L-Histidine (Sigma-Aldrich, catalog #H8000), L-Histidin monohydro-chloride monohydrate (Sigma-Aldrich, catalog #H8125) and sodium chloride (Sigma-Aldrich, catalog #S5886).

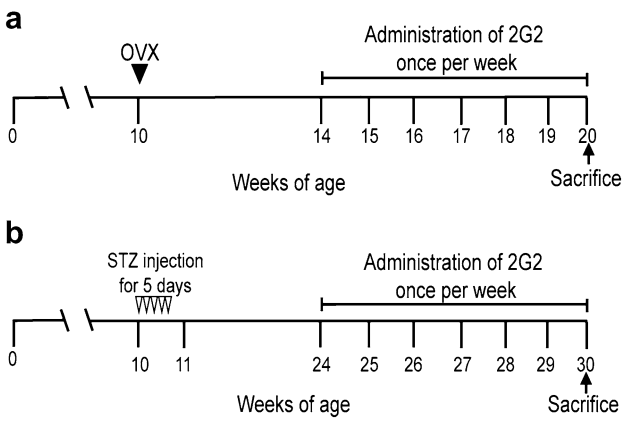

Fig. 1 Experimental design for the evaluation of the anti-resorptive effect of anti-CSF-1R antibody. Murine models of (**a**) primary osteoporosis (ovariectomy, OVX) and (**b**) secondary osteoporosis (streptozotocin-induced type-1 diabetes; STZ-T1D)

Statistical analysis

All values are presented as mean ± standard error of the mean (SEM). A one-way analysis of variance (ANOVA) followed by Student–Newman–Keuls post hoc test was used to compare each parameter between the different experimental groups. Significance level was set at $p < 0.05$. Statistical comparisons were performed using Sigma Plot software V12.0.

Results

Effect of 2G2 antibody on body weight in an OVX model

Chronic administration (10 mg/kg; once per week for 6 weeks) of anti-CSF-1R (2G2) did not significantly affect the body weight between different experimental groups (37.31 ± 2.03 g in OVX mice treated with vehicle *vs* 39.76 ± 2.10 g in OVX mice treated with 2G2 antibody). At sacrifice time (10 weeks after OVX), the body weight was not statistically different between sham mice vs OVX mice (36.04 ± 1.59 g in sham mice vs 37.31 ± 2.03 g in OVX mice). The reason why OVX did not induce a body weight gain in ICR mice is unclear; however, it is possible that strain of mice may explain this observation. In support of this, a significant increase in body weight has been reported after OVX in C3H/HeJ mice, but not in BALB/cByJ, CAST/EiJ, DBA2/J, and C57BL/6 J mice [30].

Effect of 2G2 antibody on trabecular bone of distal femur and proximal tibia in an OVX model

Figure 2 shows representative images of longitudinal views of the femur from naïve group (Fig. 2a), sham group treated with vehicle (Veh) (Fig. 2b), OVX group treated with vehicle (Fig. 2c) and OVX mice treated with 2G2 antibody (Fig. 2d) at 10 weeks post-OVX surgery. Sham surgery itself did not modify the trabeculae as compared to age-matched naïve group. In contrast, OVX induced a significant loss of trabecular bone as compared to sham group. Chronic treatment for 6 weeks with a 2G2 antibody (10 mg/kg) reversed the OVX-induced trabecular bone loss in the femur. Quantitative trabecular bone analysis at the distal femoral metaphysis and proximal tibial metaphysis revealed that sham group had similar values in magnitude of tBMD (Figs. 2e, 3a), BV/TV (Figs. 2f, 3b), Tb.N (Figs. 2g, 3c), and Tb.Sp (Figs. 2h, 3d) as compared to age-matched naïve group. In contrast, mice with OVX had a significantly smaller tBMD (Fig. 2c, e), BV/TV (Fig. 2c, f), Tb.N (Fig. 2c, g) and greater Tb.Sp (Fig. 2c, h) as compared to sham group at the femoral metaphysis. At the tibial metaphysis, mice with OVX had a significant smaller BV/TV (Fig. 3b) and greater Tb.Sp (Fig. 3d) as compared to mice with sham surgery. At this anatomical level, mice with OVX had smaller values of tBMD (Fig. 3a) and Tb.N (Fig. 3c) but these parameters were not statistically significant *vs* those values in sham mice ($p = 0.1728$ and 0.0637, respectively). Interestingly, chronic treatment with 2G2 antibody reversed both the OVX-induced reduction of tBMD (Fig. 2e), BV/TV (Fig. 2f), Tb.N (Fig. 2g) and OVX-induced increase of Tb.Sp (Fig. 2h) at the distal femoral metaphysis. The anti-CSF-1R treatment also reversed the OVX-induced reduction of BV/TV (Fig. 3b) and OVX-induced increase of Tb.Sp (Fig. 3d) at the proximal tibial metaphysis. Additionally, we evaluated changes in bone remodeling in the femoral neck between OVX and sham groups and there were no statistical differences in tBMD, BV/TV and Tb.N (data not shown).

Effect of 2G2 antibody on cortical bone at the femoral and tibial mid-diaphysis in an OVX model

MicroCT analysis revealed that cBMD, Ct.Th, B.Ar, T.Ar and B.Ar./T.Ar of the mid-diaphyseal femur and tibia did not show significant differences between sham and age-matched naïve groups. Additionally, OVX did not induce any significant decrease on these parameters. Chronic treatment with 2G2 antibody in OVX mice did not significantly alter these parameters (Table 1).

Effect of 2G2 antibody on body weight and glucose levels in a T1D model

In our experimental conditions, two mice out of nine mice in the group of T1D plus vehicle and one mouse out of ten mice in the group of T1D + 2G2 showed signs of distress. Then, blood glucose levels were measured, and they were above the upper limit of detection in our glucometer (600 mg/dL), thus, these mice were sacrificed. Chronic treatment with 2G2 antibody did not modify the body weight of mice after 6 weeks of treatment; mice with STZ treated with vehicle weighed 33.19 ± 1.51 g and mice with STZ treated with 2G2 antibody weighed 34.42 ± 1.31 g. Regarding serum glucose levels, chronic treatment with 2G2 antibody did not significantly modify the fasting glucose levels (526.1 ± 22.38 mg/dL) as compared to mice with T1D treated with vehicle (476.9 ± 47.85 mg/dL).

Effect of 2G2 antibody on cortical and trabecular bone of the femur in a T1D model

Analysis of the mid-diaphysis cortical bone of the femur was performed at 19 weeks after induction of T1D. Figure 4a shows a longitudinal section to illustrate where

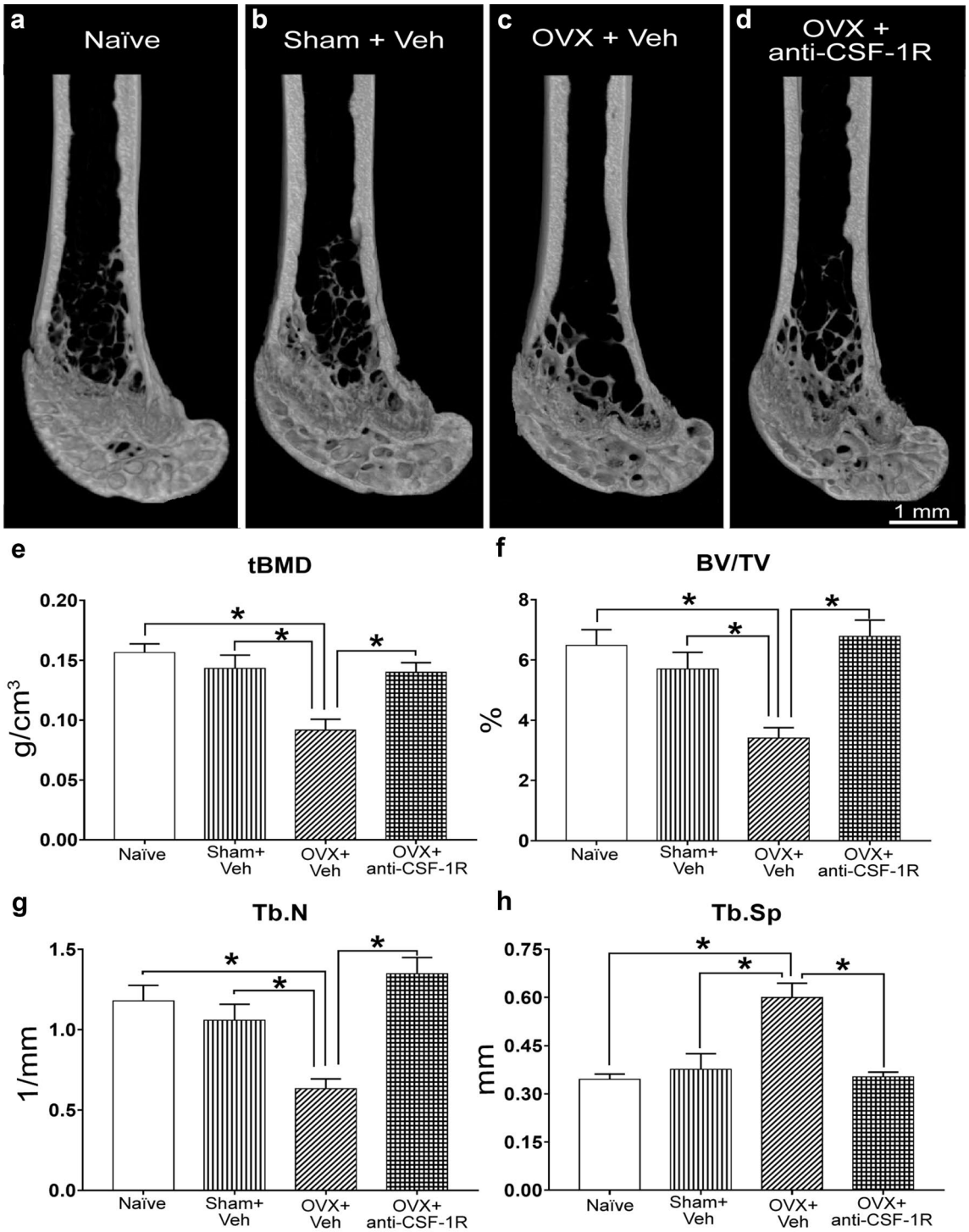

Fig. 2 The 2G2 antibody reversed the loss of trabecular bone of the distal femur in an OVX model. Representative 3D images of longitudinal distal femur sections obtained by microCT. Ovariectomy + Vehicle group (OVX + Veh) (**c**) showed significant bone loss compared to naïve (**a**) and sham groups (**b**). After the administration of anti-CSF-1R (2G2), bone loss caused by OVX was reversed (**d**). After OVX surgery, the animals showed significant bone loss in trabecular bone mineral density (tBMD) (**e**), trabecular bone volume rate (BV/TV) (**f**), trabecular number (Tb.N) (**g**), and increases in trabecular separation (Tb.Sp) (**h**) compared to naïve group. Administration of 2G2 antibody (10 mg/kg) reversed bone loss caused by the OVX model according to tBMD (**e**), BV/TV (**f**), Tb.N (**g**), and Tb.Sp (**h**) parameters. Data are presented as mean ± SEM ($n = 6$ for each group). *$p < 0.05$, data were analyzed by one-way ANOVA, followed by Student–Newman–Keuls post hoc test

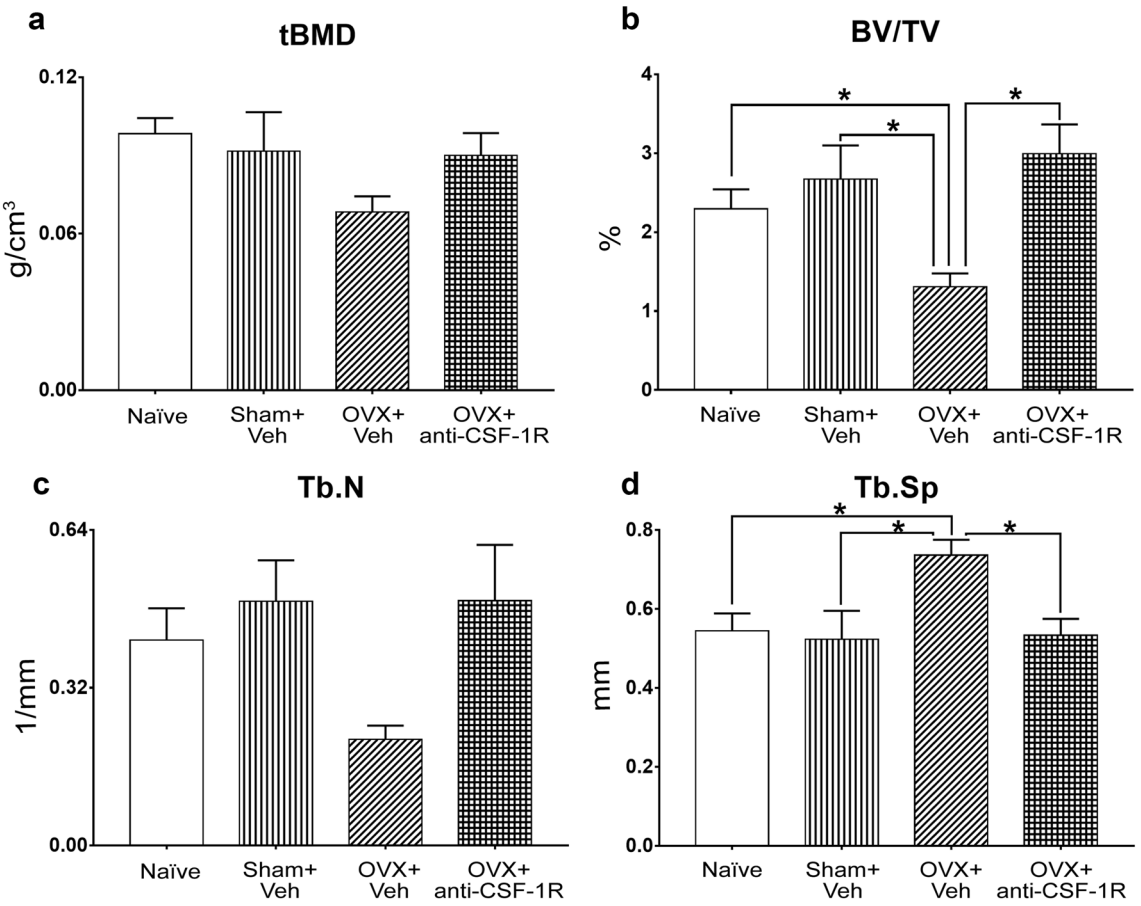

Fig. 3 The 2G2 antibody partially reversed the trabecular bone loss at the proximal tibia in an OVX model. There were no significant statistical differences among the groups in the trabecular bone mineral density (tBMD) (**a**), and trabecular number (Tb.N) (**c**) parameters. In the Ovariectomy + Vehicle (OVX + Veh) group, a significant decrease in trabecular bone volume rate (BV/TV) (**b**), and an increase in trabecular separation (Tb.Sp) (**d**) were found in comparison to naïve group. The administration of an anti-CSF-1R (2G2) antibody resulted in a significant increase in BV/TV (b), and a significant decrease in Tb.Sp (d) compared to the OVX + Veh group. Data are presented as mean ± SEM ($n = 6$ for each group). *$p < 0.05$, data were analyzed by one-way ANOVA, followed by Student–Newman–Keuls post-hoc test

Table 1 Structural parameters of cortical bone in femur and tibia in mice with primary osteoporosis

Parameters	Naïve	Sham + vehicle	OVX + vehicle	OVX + anti-CSF-1R
Cortical femur				
cBMD (g/cm^3)	1.462 ± 0.003	1.492 ± 0.013	1.477 ± 0.011	1.463 ± 0.004
Ct.Th (mm)	0.258 ± 0.019	0.253 ± 0.004	0.257 ± 0.004	0.264 ± 0.007
B.Ar (mm^2)	1.123 ± 0.052	1.034 ± 0.041	1.066 ± 0.049	1.108 ± 0.037
T.Ar (mm^2)	1.394 ± 0.059	1.299 ± 0.043	1.335 ± 0.057	1.385 ± 0.040
B.Ar/T.Ar	80.5 ± 0.454	79.57 ± 0.341	79.79 ± 0.346	79.98 ± 0.403
Cortical tibia				
cBMD (g/cm^3)	1.402 ± 0.018	1.381 ± 0.012	1.411 ± 0.013	1.423 ± 0.011
Ct.Th (mm)	0.241 ± 0.008	0.236 ± 0.006	0.240 ± 0.009	0.250 ± 0.006
B.Ar (mm^2)	0.869 ± 0.034	0.905 ± 0.037	0.889 ± 0.037	0.98 ± 0.019
T.Ar (mm^2)	1.114 ± 0.039	1.179 ± 0.042	1.153 ± 0.043	1.254 ± 0.024
B.Ar/T.Ar	77.97 ± 0.562	76.79 ± 0.505	77.06 ± 0.816	78.18 ± 0.502

cBMD bone mineral density; *Ct.Th* cortical thickness; *B.Ar* mean total cross-sectional bone area; *T.Ar* mean total cross-sectional tissue area; *B.Ar/T.Ar* mean cortical area fraction

Values are mean ± SEM ($n = 6$ for each group). *$p < 0.05$, data were analyzed by one-way ANOVA, Newman-Keuls post-hoc test

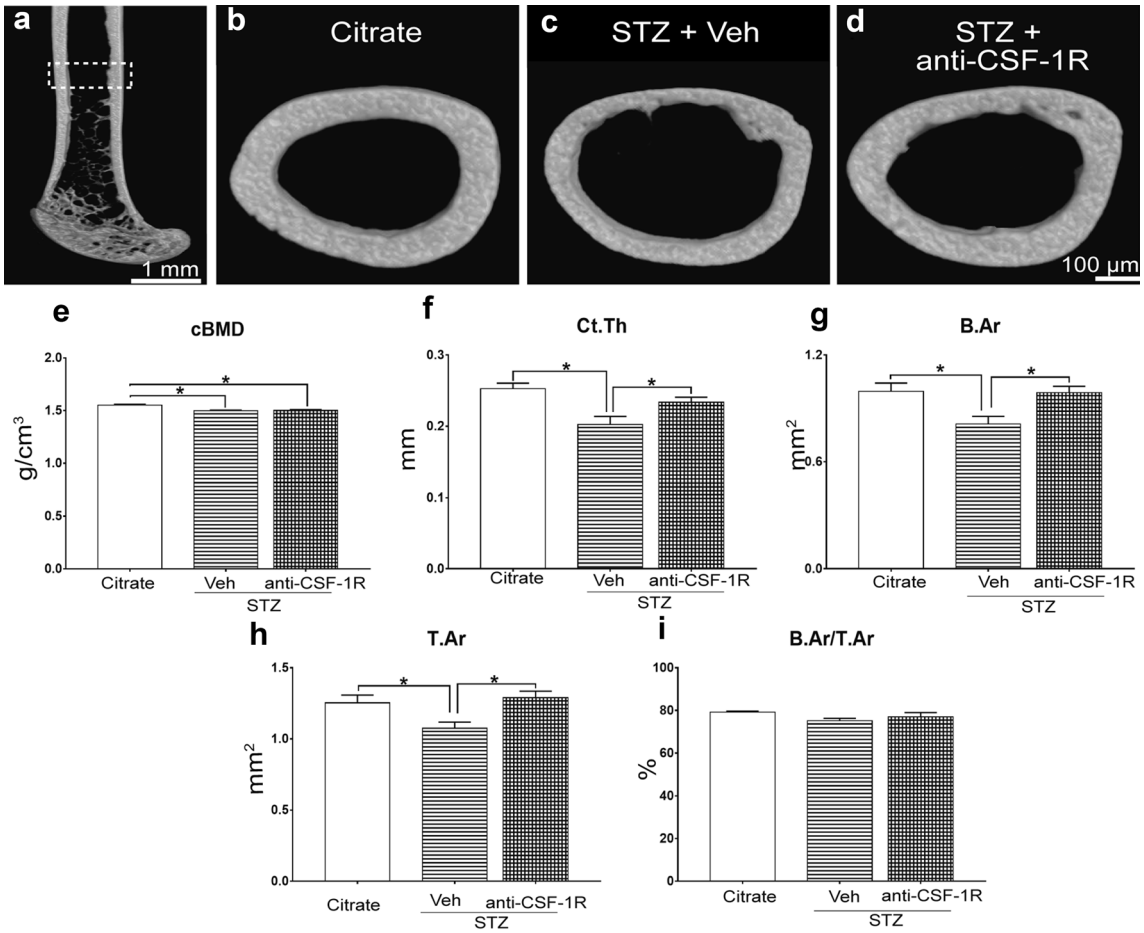

Fig. 4 The 2G2 antibody reversed cortical bone loss in a T1D model. Three-dimensional longitudinal image section of distal femur (**a**), transverse sections of femoral cortical bone (**b**, **c**, **d**) obtained by microCT analysis. The quantifications show that mice with type-1 diabetes (T1D) induced by streptozotocin (STZ) had significant loss in cortical bone mineral density (cBMD) (**e**), cortical thickness (Ct. Th) (**f**), mean cross-sectional bone area (B.Ar) (**g**), and mean total cross-sectional tissue area (T.Ar) (**h**), but not in the mean cortical area fraction (B.Ar/T.Ar) (**i**) as compared to citrate group. The administration of an anti-CSF-1R (2G2) antibody reversed the loss of cortical thickness (**f**), mean cross-sectional bone area (**g**), and mean cross-sectional tissue area (**h**) in secondary osteoporosis (STZ-induced T1D) model. Data are presented as mean ± SEM ($n = 7–9$ for each group). *$p < 0.05$, data were analyzed by one-way ANOVA, followed by Student–Newman–Keuls post hoc test

the analysis was performed. Mice with STZ-induced T1D had a thinner cortical thickness and cortical area (Fig. 4c) as compared to citrate group (control) (Fig. 4b). Chronic treatment with 2G2 antibody in the STZ-induced T1D for 6 weeks reversed the deterioration of cortical bone (Fig. 4d). Quantitative analysis revealed that STZ-induced T1D significantly reduced the cBMD (Fig. 4e), Ct.Th (Fig. 4f), B.Ar (Fig. 4g), T.Ar (Fig. 4h) but not the B.Ar/T.Ar (Fig. 4i) as compared to citrate group. The 2G2 antibody treatment only significantly reversed the T1D-induced reduction of Ct.Th, B.Ar and T.Ar but not the cBMD. When the trabecular bone was analyzed at the distal metaphysis (Fig. 5a), STZ-induced T1D did not reduce the tBMD (Fig. 5c, e), BV/TV (Fig. 5c, f), or Tb.N (Fig. 5c, g). Surprisingly, mice with STZ-induced T1D and treated with 2G2 antibody showed a greater tBMD (Fig. 5d, e), BV/TV (Fig. 5f), and Tb.N (Fig. 5g) as compared to control mice (citrate group, Fig. 5b).

Effect of 2G2 antibody on trabecular bone of femoral neck in a T1D model

Figure 6a shows a longitudinal section to illustrate where the analysis was performed. Mice with STZ-induced T1D and treated with vehicle (Veh) had a loss of trabecular bone as reflected by a smaller number and greater separation of trabeculae (Fig. 6c) as compared to control group (Fig. 6b). Six weeks of treatment with 2G2 antibody partially reversed the deterioration of trabecular bone at femoral neck (Fig. 6d). Quantitative analysis revealed that mice with STZ-induced T1D had a significantly smaller tBMD (Fig. 6e), BV/TV (Fig. 6f), and greater Tb.Sp (Fig. 6h) as compared to

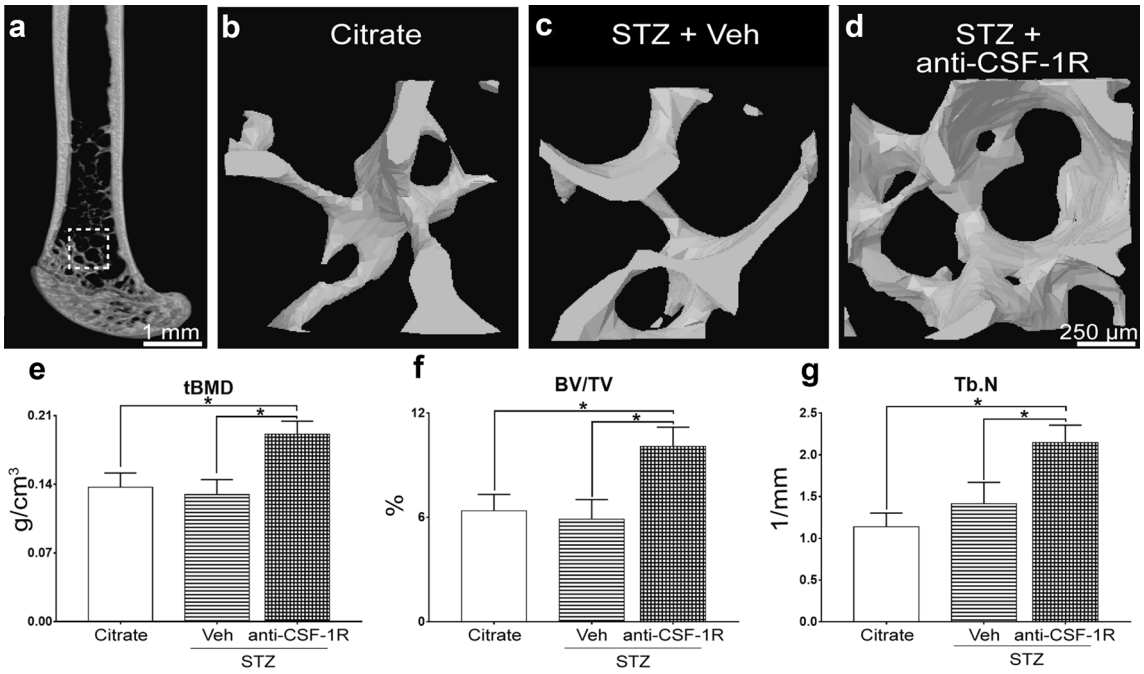

Fig. 5 Effect 2G2 antibody on femoral trabecular bone of mice with T1D. Three-dimensional longitudinal image section of distal femur (**a**), and high power magnifications of the areas analyzed (**b**, **c**, **d**). In the trabecular analysis, no significant differences among trabecular bone mineral density tBMD (**e**), trabecular bone volume rate (BV/TV) (**f**) or trabecular number (Tb.N) (**g**) were found in the streptozotocin (STZ) group compared to the citrate group. The group administered anti-CSF-1R (2G2) showed a significant increase in tBMD (**e**), BV/TV (**f**), and Tb.N (**g**) compared to vehicle (Veh) group. Data are presented as mean ± SEM ($n = 7$–9 for each group). *$p < 0.05$, data were analyzed by one-way ANOVA, followed by Student–Newman–Keuls post-hoc test

citrate group. In the Tb.N parameter, only a light trend was observed in the STZ-induced T1D. Chronic treatment with 2G2 antibody partially reversed the T1D-induced decrease of tBMD and BV/TV. However, this antibody did not reverse the T1D-induced increase of Tb.Sp.

Effect of 2G2 antibody on cortical and trabecular bone of naïve mice

The chronic administration of 2G2 antibody in age-matched naïve mice tended to increase the parameters of trabecular bone of the distal femur and proximal tibia (with exception of tibial tBMD and femoral Tb.N, in where there was a significant increase, Table 2) as compared to naïve mice. The antibody 2G2 did not significantly alter the parameters of cortical bone of the distal femur or proximal tibia or the trabecular bone at the femoral neck (Table 2).

Discussion

It has been recently reported that regulation of the CSF-1/CSF-1R signaling pathway is more complex than previously thought, as CSF-1 has at least three different isoforms; membrane-bound (mCSF-1), soluble (sCSF-1) and "shed" CSF-1, all which bind to CSF-1R [19, 31–33]. Furthermore, recent studies have identified IL-34 as a novel ligand of the CSF-1R [33, 34]. IL-34 and CSF-1 bind to partially different binding sites on CSF-1R and have a complementary, but not redundant activation of CSF-1R [18]. Thus, blockade of the receptor, instead of ligands, could offer an alternative and likely a more effective way to inhibit the CSF-1/CSF-1R pathway. While a previous study showed that neutralization of CSF-1 prevented the loss of cortical bone density (DEXA evaluation) induced by OVX [23], the present study shows that blockade of the CSF-1R reverses not only the loss of cortical bone density but also restores the microarchitecture of trabecular bone in two different mouse models of osteoporosis (primary and secondary) using highly sensitive microCT analysis. Our study is in agreement with a very recently study in which a CSF-1R inhibitor can protect against LPS-induced bone loss and deterioration of bone biomechanical properties by inhibiting osteoclast formation [24].

Our data show that chronic treatment with antibody against CSF-1R (2G2) reverted the OVX-induced loss of the trabecular bone at the distal femur and proximal tibia. While the mechanism behind this effect was not examined in the current study, we suggest, based on previous reports that this effect could result from a blockade of osteoclastogenesis and

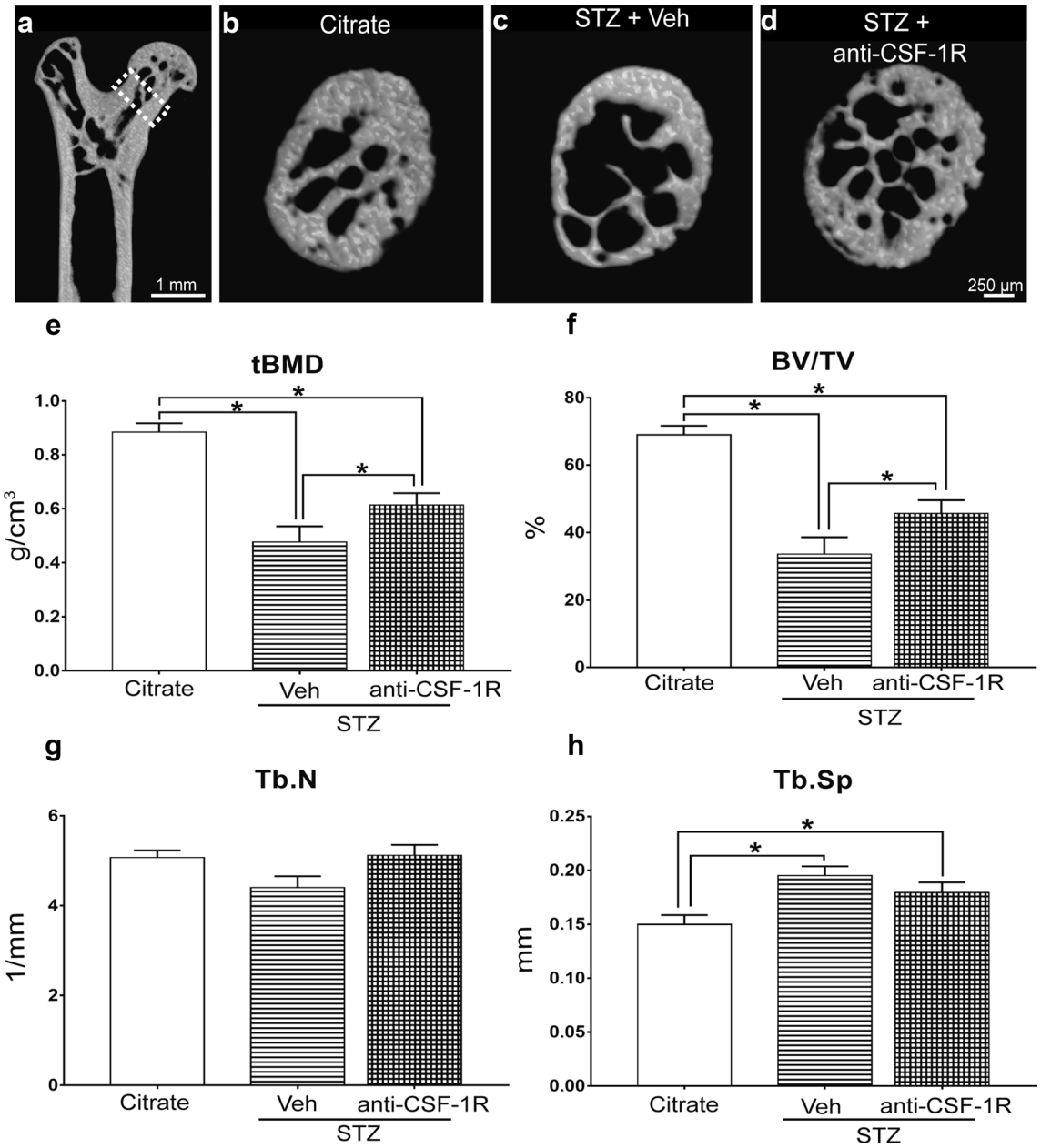

Fig. 6 The 2G2 antibody partially reversed bone loss at the femoral neck in a mouse T1D model. Longitudinal section of proximal femur (**a**), transverse sections of femoral neck (**b**–**d**) obtained by microCT analysis. Mice with streptozotocin (STZ)-induced T1D had a significant decrease in trabecular bone mineral density (tBMD) (**e**), trabecular bone volume rate (BV/TV) (**f**), and an increase in the trabecular separation (Tb.Sp) (**h**), but no significant changes in the trabecular number (Tb.N) (**g**) compared to citrate group. The administration of an anti-CSF-1R (2G2) antibody partially relieved the loss of tBMD (**e**), and BV/TV (**f**) but it did not reduce the increase in Tb.Sp (**h**) compared to vehicle (Veh) group. Data are presented as mean ± SEM ($n = 7$–9 for each group). *$p < 0.05$, data were analyzed by one-way ANOVA, followed by Student–Newman–Keuls post hoc test

osteoclast reabsorbing activity mediated by CSF-1/CSF-1R pathway. First, clinical and preclinical studies have shown that estrogen-deficiency bone loss results mainly from increased osteoclast number and bone reabsorbing activity [35, 36]. Second, in vitro studies have shown increased levels of both CSF-1 mRNA and protein by stromal cells isolated from mice with OVX and a direct relationship between CSF-1 levels and osteoclasts production [37, 38]. Third, in vivo studies have shown that genetic deletion of CSF-1 or neutralizing antibody to CSF-1 prevents the OVX-induced bone loss in mice [19, 23, 39]. Finally, women with late menopause (≥ 30 years after menopause) have significant increased levels of CSF-1 as compared to women in the premenopausal stage [40] and protein levels of CSF-1

Table 2 Structural parameters of trabecular and cortical bone in femoral neck, distal femur and proximal tibia in intact mice

ROI	Parameters	Naïve ($n=7$)	Naïve + anti-CSF-1R ($n=7$)
Trabecular femoral neck	tBMD (g/cm^3)	0.771 ± 0.033	0.816 ± 0.041
	BV/TV (%)	60.07 ± 2.958	64.99 ± 4.008
	Tb.N (1/mm)	5.832 ± 0.154	5.513 ± 0.367
	Tb.Sp (mm)	0.126 ± 0.009	0.137 ± 0.011
Trabecular distal femur	tBMD (g/cm^3)	0.155 ± 0.006	0.207 ± 0.030
	BV/TV (%)	6.498 ± 0.436	11.16 ± 2.315
	Tb.N (1/mm)	1.018 ± 0.181	1.942 ± 0.3647*
	Tb.Sp (mm)	0.344 ± 0.014	0.301 ± 0.025
Cortical distal femur	cBMD (g/cm^3)	1.464 ± 0.028	1.47 ± 0.016
	Ct.Th (mm)	0.279 ± 0.017	0.259 ± 0.008
	B.Ar (mm^2)	1.113 ± 0.045	1.048 ± 0.047
	T.Ar (mm^2)	1.387 ± 0.050	1.313 ± 0.052
	B.Ar/T.Ar	80.21 ± 0.482	79.74 ± 0.512
Trabecular proximal tibia	tBMD (g/cm^3)	0.098 ± 0.004	0.141 ± 0.017*
	BV/TV (%)	2.426 ± 0.247	5.419 ± 1.284
	Tb.N (1/mm)	0.447 ± 0.062	0.931 ± 0.261
	Tb.Sp (mm)	0.531 ± 0.039	0.421 ± 0.038
Cortical proximal tibia	cBMD (g/cm^3)	1.406 ± 0.016	1.394 ± 0.012
	Ct.Th (mm)	0.244 ± 0.007	0.245 ± 0.005
	B.Ar (mm^2)	0.884 ± 0.033	0.927 ± 0.031
	T.Ar (mm^2)	1.136 ± 0.040	1.196 ± 0.035
	B.Ar/T.Ar	77.82 ± 0.498	77.48 ± 0.394

BMD bone mineral density; *BV/TV* bone volume fraction; *Tb.N* trabecular number; *Tb.Sp* trabecular separation; *Ct.Th* cortical thickness; *B.Ar* mean total cross-sectional bone area; *T.Ar* mean total cross-sectional tissue area; *B.Ar/T.Ar* mean cortical area fraction

Values are mean ± SEM. *$p < 0.05$, data were analyzed by Student's *t* test

in the femoral head are significantly higher in patients with osteoporotic-related fractures than in patients with osteoarthritis [41].

Osteoporosis is not only a major public health problem in postmenopausal women or aged people but also in premenopausal women as a consequence of treatment and/or chronic disease such as diabetes. Both T1D and T2D have been reported to increase risk of fracture; however, T1D has a stronger association with hip fracture (summary relative risk of 6.3) than T2D (summary relative risk of 1.7) [12]. In our study, we showed that mice with T1D have a significant cortical bone loss at the distal femur and neck of the femur (an anatomical site where hip fractures occur) and that blockade of CSF-1R reverts partially the loss of cortical bone in the distal femur and femoral neck, suggesting that an increased activation of the CSF-1/CSF-1R pathway is also involved in the bone loss by T1D. In support of this hypothesis, both the levels of mRNA and protein for CSF-1 and its receptor, CSF-1R are significantly higher in retina from rats with T1D as compared to age-matched naïve rats [38]. However, it should be recognized that we did not determine the levels or expression of CSF-1 or its receptor, in bone tissue. Future studies are needed to determine serum and/or bone levels of CSF-1 and its receptor as well as the pattern of expression of these proteins in bone tissue under T1D conditions. The observation that mice with STZ-induced T1D did not show trabecular bone loss in the femoral metaphysis was somewhat surprising given the evidence that bone loss in these mice occurred even at femoral cortical bone. The reasons behind this observation are unknown; however, the strain of mice could explain why these mice are ¨resistant¨ to trabecular bone loss at the distal femur induced by STZ. In support of this, it has been reported that the diabetogenic effects of STZ in mice are strain dependent [42] and that magnitude of trabecular bone loss at the femoral metaphysis in a model of disuse osteoporosis is influenced by the mouse strain [43]. Our results show that the model of T1D results in a greater loss of cortical bone compared to OVX model. These results are in agreement with previous studies which have reported that OVX performed in C57BL6 and BALB/c mice did not induce a loss of the tibial cortical bone even at prolonged times (24 weeks) after OVX [44]. In contrast, several studies have shown that mice with STZ-induced T1D display a significant loss of both trabecular and cortical bone [14, 45]. The

mechanisms underlying these model-related differences are not fully known. However, it has been suggested that T1D-induced bone loss is more severe compared to OVX-induced bone loss due to, at least in part, that T1D negatively affects both bone formation and bone reabsorption, in contrast, the OVX-induced bone loss results mainly from an increased bone reabsorption [46].

On the other hand, the microCT analysis revealed that treatment with 2G2 antibody in naïve mice tended to increase the trabecular bone at the proximal metaphysis tibia and distal metaphysis femur but not in the cortical bone of the tibia, femur and trabecular femoral neck. According to this, a significant increase in the density of trabecular bone in the femur has been previously reported in mice lacking this receptor [47]. The reasons behind the bone regional differences in terms of response to this antibody are unknown, but possibly relates to the femoral neck having a relatively lower rate of bone turnover than trabecular bone in the distal femur and proximal tibia. Another explanation could relate to periosteal modeling that is less pronounced at the femoral neck compared to the femoral or tibial midshafts [48].

Our study has several limitations. First, the mechanisms behind the anti-osteoporotic effect of the 2G2 antibody were not fully explored. Thus, future studies evaluating the effect of this drug on osteoclastogenesis and reabsorbing activity as well as on osteoblastogenesis and/or bone formation are needed. Second, we did not validate the antibody effect on osteoclast activity or density. While a previous study demonstrated that a different anti-CSF-1R antibody decreases the number of osteoclasts [49], we do not have direct evidence for the effect of the 2G2 antibody on osteoclast number and/or activity. Our rationale for using this antibody was based on the study by Ries C et al., 2014 (who kindly provided us the antibody) that reported a high affinity ($K_D = 0.2$ nM) of the 2G2 antibody binding to mouse CSF-1R, which is essential for the development and maturation of osteoclasts, and reduces the survival of CSF-1-dependent murine M-NFS-60 cells (an in vitro model of bone marrow precursors) [29]. Third, while our results show that blocking the CSF-1/CSF-1R axis reverts the loss of cortical and trabecular bone in two murine models of osteoporosis, it is unknown if pharmacological blockade of this pathway will also improve the mechanical properties of bone and thus increase the bone's resistance to fracture. Finally, a possible effect of the anti-CSF-1R antibody on disease progression in the T1D was not explored. However, our results show that T1D mice treated with anti-CSF-1R have similar values of body weight and serum glucose compared to T1D mice treated with vehicle. Additionally, it is important to mention that we did not measure potential side effects of anti-CSF-1R treatment, although normal histology in various tissues has been reported after chronic administration of this antibody in mice [50].

Conclusions

In summary, chronic treatment with an anti-CSF-1R antibody (2G2) significantly reversed the bone loss observed in mouse models of primary and secondary osteoporosis. Our results suggest that CSF-1/CSF-1R may play a key role in the bone loss induced by estrogen deficiency and T1D. Further studies elucidating the cellular mechanisms behind the anti-osteoporotic effects of CSF-1R blockade will increase our understanding of the pathogenesis of osteoporosis.

Acknowledgements This work was supported by the Consejo Nacional de Ciencia y Tecnología (the Mexican Nacional Council for Science and Technology) [CB-2014 240829, PDCPN-2015-01-191, and Apoyo para Actividades Científicas, Tecnológicas y de Innovación 2019-299535]. We deeply acknowledge to Carola H. Ries for her helpful support to achieve the antibody donation.

Author contributions JMJA, EMI and MBRR conceived the project. AMM, EMI, HFTR and MBRR performed the experiments. JMJA, RIAG and MBRR analyzed and interpreted the data. JMJA, AMM, EMI, MBRR, RIAG and HFTR wrote and edited the manuscript. All authors have read and approved the manuscript. JMJA obtained grant funding.

Compliance with ethical standards

Conflict of interest The authors declare that the research was conducted in the absence of any commercial or financial relationships that could be construed as a potential conflict of interest.

References

1. Watts NB, Investigators G. Insights from the Global Longitudinal Study of Osteoporosis in Women (GLOW). Nat Rev Endocrinol. 2014;10(7):412–22.
2. Wright NC, Looker AC, Saag KG, Curtis JR, Delzell ES, Randall S, et al. The recent prevalence of osteoporosis and low bone mass in the United States based on bone mineral density at the femoral neck or lumbar spine. J Bone Miner Res. 2014;29(11):2520–6.
3. Khosla S, Hofbauer LC. Osteoporosis treatment: recent developments and ongoing challenges. Lancet Diabetes Endocrinol. 2017;5(11):898–907.
4. Lutz W, Sanderson W, Scherbov S. The coming acceleration of global population ageing. Nature. 2008;451(7179):716–9.
5. Valderrabano RJ, Linares MI. Diabetes mellitus and bone health: epidemiology, etiology and implications for fracture risk stratification. Clin Diabetes Endocrinol. 2018;4:9.
6. Teitelbaum SL, Ross FP. Genetic regulation of osteoclast development and function. Nat Rev Genet. 2003;4(8):638–49.
7. Stanley ER, Berg KL, Einstein DB, Lee PS, Pixley FJ, Wang Y, et al. Biology and action of colony–stimulating factor-1. Mol Reprod Dev. 1997;46(1):4–10.
8. Ji MX, Yu Q. Primary osteoporosis in postmenopausal women. Chronic Dis Transl Med. 2015;1(1):9–13.
9. Eastell R, O'Neill TW, Hofbauer LC, Langdahl B, Reid IR, Gold DT, et al. Postmenopausal osteoporosis. Nat Rev Dis Primers. 2016;2:16069.

10. Riggs BL, Wahner HW, Dunn WL, Mazess RB, Offord KP, Melton LJ 3rd. Differential changes in bone mineral density of the appendicular and axial skeleton with aging: relationship to spinal osteoporosis. J Clin Invest. 1981;67(2):328–35.
11. Neumann T, Lodes S, Kastner B, Lehmann T, Hans D, Lamy O, et al. Trabecular bone score in type 1 diabetes a cross-sectional study. Osteoporos Int. 2016;27(1):127–33.
12. Janghorbani M, Van Dam RM, Willett WC, Hu FB. Systematic review of type 1 and type 2 diabetes mellitus and risk of fracture. Am J Epidemiol. 2007;166(5):495–505.
13. Hough FS, Pierroz DD, Cooper C, Ferrari SL, Bone IC, Diabetes WG. Mechanisms in endocrinology: mechanisms and evaluation of bone fragility in type 1 diabetes mellitus. Eur J Endocrinol. 2016;174(4):R127–R138138.
14. Botolin S, Faugere MC, Malluche H, Orth M, Meyer R, McCabe LR. Increased bone adiposity and peroxisomal proliferator-activated receptor-gamma2 expression in type I diabetic mice. Endocrinology. 2005;146(8):3622–31.
15. Kayal RA, Tsatsas D, Bauer MA, Allen B, Al-Sebaei MO, Kakar S, et al. Diminished bone formation during diabetic fracture healing is related to the premature resorption of cartilage associated with increased osteoclast activity. J Bone Miner Res. 2007;22(4):560–8.
16. Stanley ER, Berg KL, Einstein DB, Lee PS, Yeung YG. The biology and action of colony stimulating factor. Stem Cells. 1994;12:15–24.
17. Pollard JW. Trophic macrophages in development and disease. Nat Rev Immunol. 2009;9(4):259–70.
18. El-Gamal MI, Al-Ameen SK, Al-Koumi DM, Hamad MG, Jalal NA, Oh CH. Recent advances of colony-stimulating factor-1 receptor (CSF-1R) kinase and its inhibitors. J Med Chem. 2018;61(13):5450–66.
19. Yao GQ, Wu JJ, Troiano N, Zhu ML, Xiao XY, Insogna K. Selective deletion of the membrane-bound colony stimulating factor 1 isoform leads to high bone mass but does not protect against estrogen-deficiency bone loss. J Bone Miner Metab. 2012;30(4):408–18.
20. Pixley FJ, Stanley ER. CSF-1 regulation of the wandering macrophage: complexity in action. Trends Cell Biol. 2004;14(11):628–38.
21. Harris SE, MacDougall M, Horn D, Woodruff K, Zimmer SN, Rebel VI, et al. Meox2Cre-mediated disruption of CSF-1 leads to osteopetrosis and osteocyte defects. Bone. 2012;50(1):42–53.
22. Saini A, Liu YJ, Cohen DJ, Ooi BS. Hyperglycemia augments macrophage growth responses to colony-stimulating factor-1. Metabolism. 1996;45(9):1125–9.
23. Cenci S, Weitzmann MN, Gentile MA, Aisa MC, Pacifici R. M-CSF neutralization and egr-1 deficiency prevent ovariectomy-induced bone loss. J Clin Invest. 2000;105(9):1279–87.
24. Wang XF, Wang YJ, Li TY, Guo JX, Lv F, Li CL, et al. Colony-stimulating factor 1 receptor inhibition prevents against lipopolysaccharide -induced osteoporosis by inhibiting osteoclast formation. Biomed Pharmacother. 2019;115:108916.
25. Enriquez-Perez IA, Galindo-Ordonez KE, Pantoja-Ortiz CE, Martinez-Martinez A, Acosta-Gonzalez RI, Munoz-Islas E, et al. Streptozocin-induced type-1 diabetes mellitus results in decreased density of CGRP sensory and TH sympathetic nerve fibers that are positively correlated with bone loss at the mouse femoral neck. Neurosci Lett. 2017;655:28–34.
26. Vargas-Munoz VM, Martinez-Martinez A, Munoz-Islas E, Ramirez-Rosas MB, Acosta-Gonzalez RI, Jimenez-Andrade JM. Chronic administration of Cl-amidine, a pan-peptidylarginine deiminase inhibitor, does not reverse bone loss in two different murine models of osteoporosis. Drug Dev Res. 2020;81(1):93–101.
27. Zhang Y, Cheng N, Miron R, Shi B, Cheng X. Delivery of PDGF-B and BMP-7 by mesoporous bioglass/silk fibrin scaffolds for the repair of osteoporotic defects. Biomaterials. 2012;33(28):6698–708.
28. Bouxsein ML, Boyd SK, Christiansen BA, Guldberg RE, Jepsen KJ, Muller R. Guidelines for assessment of bone microstructure in rodents using micro-computed tomography. J Bone Miner Res. 2010;25(7):1468–86.
29. Ries CH, Cannarile MA, Hoves S, Benz J, Wartha K, Runza V, et al. Targeting tumor-associated macrophages with anti-CSF-1R antibody reveals a strategy for cancer therapy. Cancer Cell. 2014;25(6):846–59.
30. Bouxsein ML, Myers KS, Shultz KL, Donahue LR, Rosen CJ, Beamer WG. Ovariectomy-induced bone loss varies among inbred strains of mice. J Bone Miner Res. 2005;20(7):1085–92.
31. Bazan JF. Genetic and structural homology of stem cell factor and macrophage colony-stimulating factor. Cell. 1991;65(1):9–10.
32. Miyazawa K, Williams DA, Gotoh A, Nishimaki J, Broxmeyer HE, Toyama K. Membrane-bound Steel factor induces more persistent tyrosine kinase activation and longer life span of c-kit gene-encoded protein than its soluble form. Blood. 1995;85(3):641–9.
33. Ladner MB, Martin GA, Noble JA, Nikoloff DM, Tal R, Kawasaki ES, et al. Human CSF-1: gene structure and alternative splicing of mRNA precursors. EMBO J. 1987;6(9):2693–8.
34. Lin H, Lee E, Hestir K, Leo C, Huang M, Bosch E, et al. Discovery of a cytokine and its receptor by functional screening of the extracellular proteome. Science. 2008;320(5877):807–11.
35. Sarma U, Edwards M, Motoyoshi K, Flanagan AM. Inhibition of bone resorption by 17beta-estradiol in human bone marrow cultures. J Cell Physiol. 1998;175(1):99–108.
36. Lea CK, Sarma U, Flanagan AM. Macrophage colony stimulating-factor transcripts are differentially regulated in rat bone-marrow by gender hormones. Endocrinology. 1999;140(1):273–9.
37. Kimble RB, Srivastava S, Ross FP, Matayoshi A, Pacifici R. Estrogen deficiency increases the ability of stromal cells to support murine osteoclastogenesis via an interleukin-1and tumor necrosis factor-mediated stimulation of macrophage colony-stimulating factor production. J Biol Chem. 1996;271(46):28890–7.
38. Liu W, Xu GZ, Jiang CH, Da CD. Expression of macrophage colony-stimulating factor (M-CSF) and its receptor in streptozotocin-induced diabetic rats. Curr Eye Res. 2009;34(2):123–33.
39. Yao GQ, Wu JJ, Ovadia S, Troiano N, Sun BH, Insogna K. Targeted overexpression of the two colony-stimulating factor-1 isoforms in osteoblasts differentially affects bone loss in ovariectomized mice. Am J Physiol Endocrinol Metab. 2009;296(4):E714–E720720.
40. Kamada M, Irahara M, Maegawa M, Ohmoto Y, Takeji T, Yasui T, et al. Postmenopausal changes in serum cytokine levels and hormone replacement therapy. Am J Obstet Gynecol. 2001;184(3):309–14.
41. D'Amelio P, Roato I, D'Amico L, Veneziano L, Suman E, Sassi F, et al. Bone and bone marrow pro-osteoclastogenic cytokines are up-regulated in osteoporosis fragility fractures. Osteoporos Int. 2011;22(11):2869–77.
42. Luo J, Quan J, Tsai J, Hobensack CK, Sullivan C, Hector R, et al. Nongenetic mouse models of non-insulin-dependent diabetes mellitus. Metabolism. 1998;47(6):663–8.
43. Judex S, Garman R, Squire M, Busa B, Donahue LR, Rubin C. Genetically linked site-specificity of disuse osteoporosis. J Bone Miner Res. 2004;19(4):607–13.
44. Roberts BC, Giorgi M, Oliviero S, Wang N, Boudiffa M, Dall'Ara E. The longitudinal effects of ovariectomy on the morphometric, densitometric and mechanical properties in the murine tibia: a comparison between two mouse strains. Bone. 2019;127:260–70.

45. Martin LM, McCabe LR. Type I diabetic bone phenotype is location but not gender dependent. Histochem Cell Biol. 2007;128(2):125–33.
46. Raehtz S, Bierhalter H, Schoenherr D, Parameswaran N, McCabe LR. Estrogen deficiency exacerbates type 1 diabetes-induced bone tnf-alpha expression and osteoporosis in female mice. Endocrinology. 2017;158(7):2086–101.
47. Dai XM, Ryan GR, Hapel AJ, Dominguez MG, Russell RG, Kapp S, et al. Targeted disruption of the mouse colony-stimulating factor 1 receptor gene results in osteopetrosis, mononuclear phagocyte deficiency, increased primitive progenitor cell frequencies, and reproductive defects. Blood. 2002;99(1):111–20.
48. Bagi CM, DeLeon E, Ammann P, Rizzoli R, Miller SC. Histo-anatomy of the proximal femur in rats: impact of ovariectomy on bone mass, structure, and stiffness. Anat Rec. 1996;245(4):633–44.
49. Toh ML, Bonnefoy JY, Accart N, Cochin S, Pohle S, Haegel H, et al. Bone- and cartilage-protective effects of a monoclonal antibody against colony-stimulating factor 1 receptor in experimental arthritis. Arthritis Rheumatol. 2014;66(11):2989–3000.
50. MacDonald KP, Palmer JS, Cronau S, Seppanen E, Olver S, Raffelt NC, et al. An antibody against the colony-stimulating factor 1 receptor depletes the resident subset of monocytes and tissue- and tumor-associated macrophages but does not inhibit inflammation. Blood. 2010;116(19):3955–63.